SEVERAL FEATURES OF DAM BREAK WAVE DYNAMICS AT THE RESERVOIR UPSTREAM IN CASE OF A CONCRETE DAM BREAK

Bui Van Huu[1], Le Van Nghi[1]
1. Key Laboratory of River and Coastal Engineering, Vietnam Academy for Water Resources

Abstract: *When a concrete dam failure occurs, negative reverse waves often appear at upstream and positive forward waves appear at downstream. This article presents several hydrodynamic characteristics of dam break wave dynamics at the reservoir upstream in case of a concrete dam breaks. Results obtained from computational research using 3D mathematical models with the RNG k-ε turbulence flow model, show that at upstream there is a pair of negative reverse waves in front and positive waves behind.*
Keywords: *Dam break wave dynamics, concrete dam failure.*

1. INTRODUCTION

The flow characteristics after a breach were studied very early with the works of Ritter [14], which gave a relatively comprehensive description of the 3 stages of flow development upon dam breach on a flat bottom rectangular prismatic canal with smooth and waterless downstream channel flow (Figure 2).

In development of Ritter's works, Stoker [14] made an extension to the downstream water level. Until the 90s of the 20th century, Hunt combined the theoretical researches with Experiment on physical models and confirmed the the correctness of existing theories with the prismatic canals having bottom slopes of [6], [10], [11], [12], [13]. In recent years, Hatice Ozmen-Cagatay and Selahattin Kocaman (2010, 2012; 2020) combined physical models with digital models (CFD- Flow-3D) to observe the shape of the dam-break wave free flows on the rectangle canal in case there is or is not water in downstream. Calculations comparing Shallow Water Equations (SWEs) and Reynolds – Average Navier Stokes Equations (RANS) showed that the RANS model gave better results than the SWEs model when describing the initial shape of the wave [7], [9]; for waves reflected through solid objects, the SWEs model gave better simulation of the reflected waves than the RANS model [8].

Esmaeeli Mohsenabadi.S (2019), used the Flow-3D model to simulate the dam failure and he also used different turbulent flow models, turbulent flow model of RNG K-ε (Renormalized Group) resulted in the best simulation and was proposed to be applied to complex hydraulic problems including the problem of dam failure [4]. Today, research on dam break wave dynamics in case of a dam break continues to be researched to further improve the theories and determine wave characteristics in order to bring simulation results closer to reality. Figure 1 - Show Turbulent flow simulation options in Flow-

Receipt Date: August 29th, 2023
Review Approval Date: September 12th, 2023
Publish Approval Date: October 9th, 2023

3D.

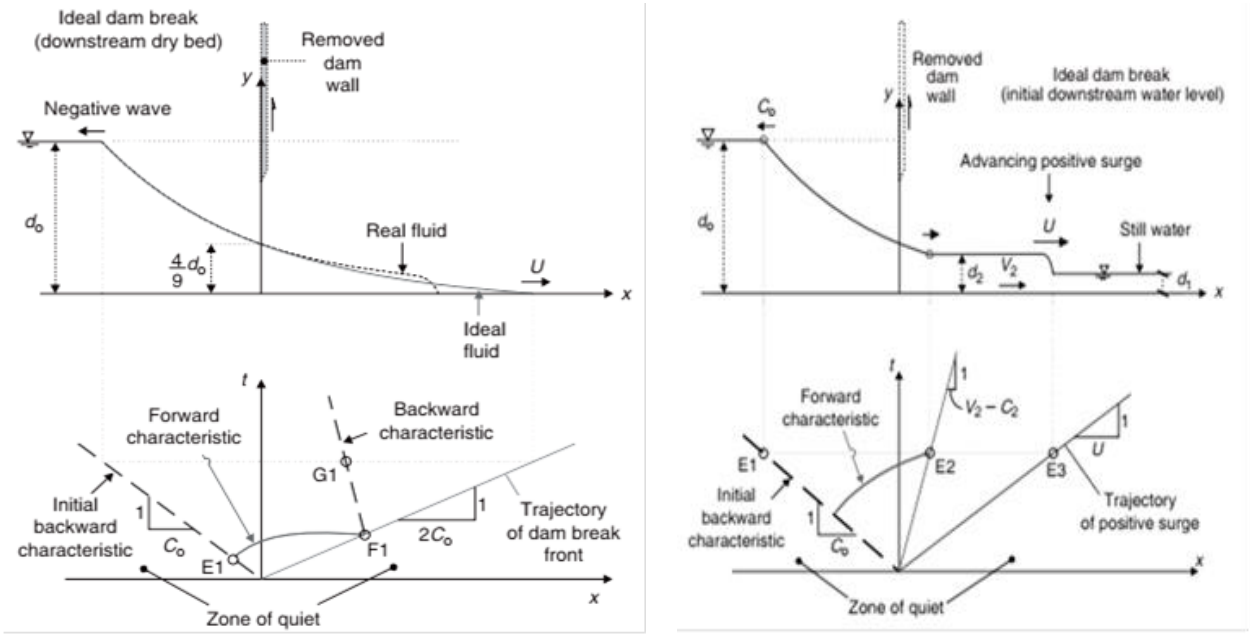

Downstream with no water

Downstream with water with $d_1 < 0{,}1383H$ (d_1- the depth of downstream waterhead)

Figure 1: Diagram of characteristics of dam-break waves on flat-bottomed channels

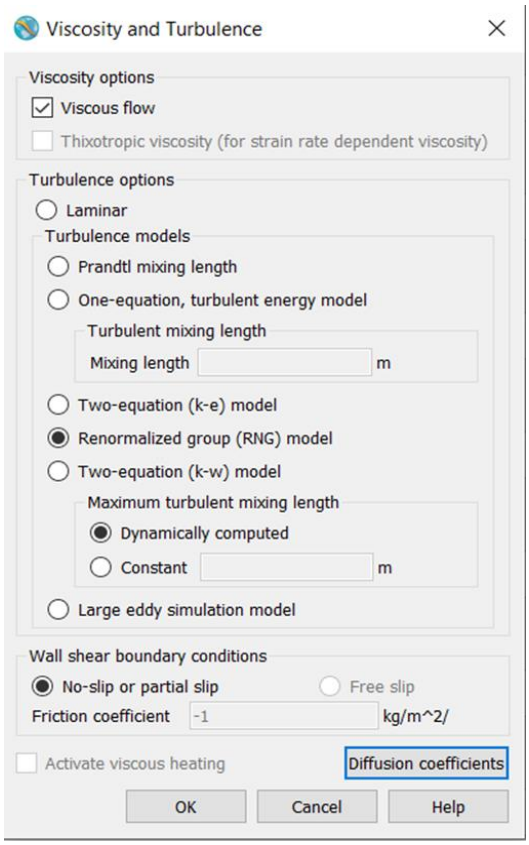

Figure 2: Turbulent flow simulation

options in Flow-3D

Although there are many studies, they only focus on the flow downstream of the breach and pay little attention to the characteristic patterns of the flow upstream of the breach (waves in the reservoir).

In this research, the researcher used digital model CFD (Flow-3D) and turbulent model RNG k-ε (Renormalization-Group Model).

2. THE DIGITAL MODEL

The digital model was established by using Flow-3D software [5], resulted in different calculating scenarios and verified by the results of physical model for a typical scenario.

2.1. Continuity equation

In the Flow-3D model, Navier-Stoke was used to describe hydrodynamic process of the flow. The 3-dimensional Navier-Stoke Equation system includes 3 momentum in the x, y and z

directions and the continuity equation is written as follows [4]:

$$\frac{\partial}{\partial x}(\rho u)+\frac{\partial}{\partial y}(\rho v)+\frac{\partial}{\partial z}(\rho w)=0$$

$$\begin{aligned}
\frac{\partial}{\partial t}(\rho u)+\frac{\partial}{\partial x}(\rho uu)+\frac{\partial}{\partial y}(\rho vu)+\frac{\partial}{\partial z}(\rho wu) &= -\frac{\partial p}{\partial x}+\mu\left(\frac{\partial^2 u}{\partial x^2}+\frac{\partial^2 u}{\partial y^2}+\frac{\partial^2 u}{\partial z^2}\right)\\
\frac{\partial}{\partial t}(\rho v)+\frac{\partial}{\partial x}(\rho uv)+\frac{\partial}{\partial y}(\rho vv)+\frac{\partial}{\partial z}(\rho wv) &= -\frac{\partial p}{\partial y}+(\vartheta+\vartheta_t)\left(\frac{\partial^2 v}{\partial x^2}+\frac{\partial^2 v}{\partial y^2}+\frac{\partial^2 v}{\partial z^2}\right)\\
\frac{\partial}{\partial t}(\rho w)+\frac{\partial}{\partial x}(\rho uw)+\frac{\partial}{\partial y}(\rho vw)+\frac{\partial}{\partial z}(\rho ww) &= -\frac{\partial p}{\partial z}+(\vartheta+\vartheta_t)\left(\frac{\partial^2 w}{\partial x^2}+\frac{\partial^2 w}{\partial y^2}+\frac{\partial^2 w}{\partial z^2}\right)
\end{aligned} \quad (1)$$

In which: **u, v, w** are the velocity components in the x, y and z directions, respectively; **ρ** is the density of the liquid; **μ** is the fluid viscosity; ϑ_t is the turbulent kinematic viscosity; **t** is time; and **p** is pressure.

The equation describing the RNG k-ε turbulent flow model is written as follows (2) (3):

$$\frac{\partial k}{\partial t}+\frac{\partial k u_i}{\partial x_i}=\frac{\partial}{\partial x_i}\left(Dk_{eff}\frac{\partial k}{\partial x_i}\right)+G_k-\varepsilon \quad (2)$$

$$\frac{\partial \varepsilon}{\partial t}+\frac{\partial \varepsilon u_i}{\partial x_i}=\frac{\partial}{\partial x_i}\left(D\varepsilon_{eff}\frac{\partial \varepsilon}{\partial x_i}\right)+(C_{1\varepsilon}-R)\frac{\varepsilon}{k}G_k-C_{2\varepsilon}\frac{\varepsilon^2}{k} \quad (3)$$

In which: some coefficients obtained from the standard model, Dk_{eff} was identified following: (4)

$$Dk_{eff}=v+\frac{v_t}{\sigma_k} \quad (4)$$

Standardized coefficient, R, was identified following (5), (6):

$$R=\frac{\eta\left(1-\frac{\eta}{\eta_0}\right)}{1+\beta\eta^3} \quad (5)$$

$$\eta=S_{ij}\frac{k}{\varepsilon} \quad (6)$$

The constants defined are C_μ=0.0845; C1ε =1.42; C2ε =1.68; σk = 0.71942; σε =0.71942; η0 = 4.38; β = 0.012.

2.2. Development of calculation model

a. Computing grid

The model was set up including 3 reservoir areas, dam (including the breach) and downstream channel, the prototype used is Son La dam, Son La province - Figure 3;

Area 1: Reservoir with dimensions of LxBxH = 750mx1500mx150m;

Area 2: Dam (including breach) with dimension of LxBxH = 1500mx15mx150m.

Area 3: Downstream channel with dimension of LxBxH = 3000mx800mx150m with roof of

m=1.0 and main channel of 500m wide.

The coordinate origin was located upstream of the dam (upstream edge of the breach);

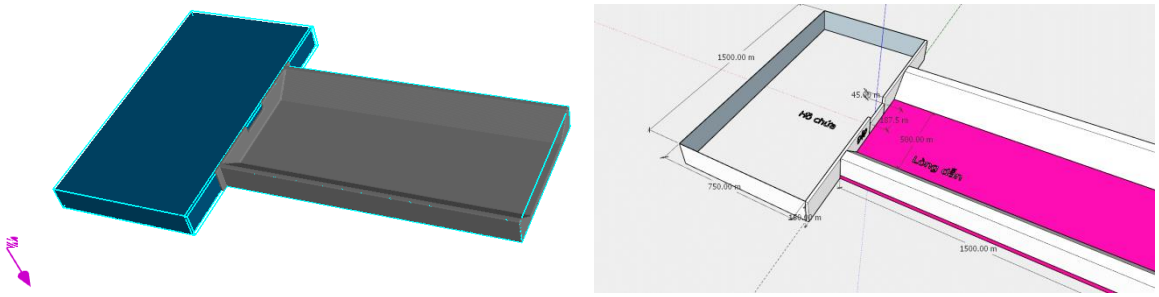

Model established on Flow-3D Dimensions of the breach

Figure 3: Model established in Flow-3D

The computing grid for the model was divided into orthogonal rectangular grid blocks with uniform grid steps: $\Delta x = \Delta y = \Delta z = 5{,}0$m.

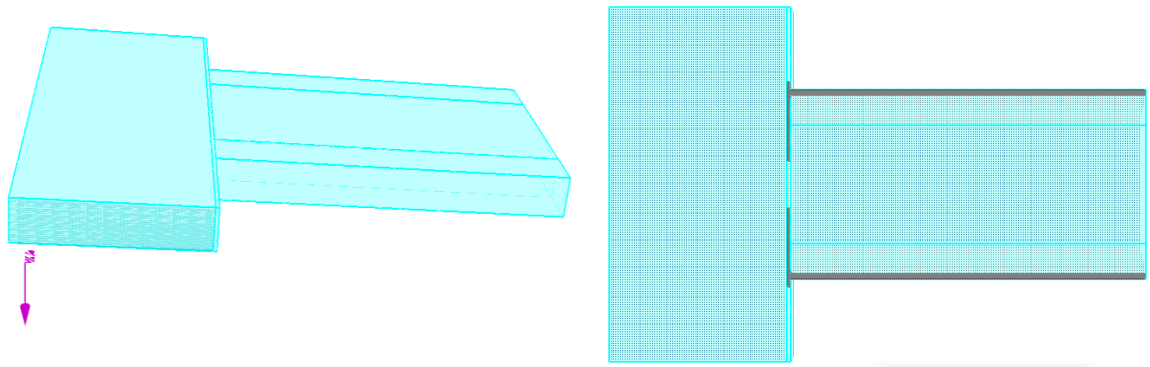

Computing grid range Computing grid surface

Figure 4: Computing grid

b. Boundary conditions of the problem

The boundary conditions of the model are imposed as shown in Figure 4, specifically:

At the inlet (reservoir's head), X_{min}=-750m, two side boundaries in terms of Y, at Y_{min} =-750m, and Y_{Max}=750m were fixed (W); at the outlet (X_{max}=3150m), the boundary was variable (O); and at the break, the boundary was pressure boundary (P).

c. Model testing

After setup, the model was tested and calibrated using data obtained from the physical model for the case that the upstream water level was 217.83m, the breach size was Bfxhf=187.5x45.0m. The calculation results are extracted and compared with the KB11 scenario [1]. The location for comparing results was at the measuring point 400m from the dam base, in the middle of the downstream channel (Table 1, Figure 6 and Figure 7). Figure 6 shows the process of water level and velocity calculated using the numerical model.

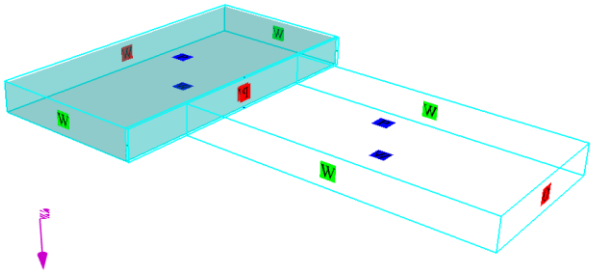

Figure 5: Boundary conditions of the model

The model testing results, according to 0, showed that the calculation error between the Flow-3D model and the experimental data on the physical model was less than 6.0%. Therefore, the Flow-3D model set for the research problem ensured reliability to calculate different scenarios for further researches.

Table1: Comparison of calculation results of the digital model and physical model

No.	Location	Wave's max height (h_w-m)		Wave's max velocity (m/s)		Time appearing The second (s)	
		Physical model	Flow-3D model	Physical model	Flow-3D model	Physical model	Flow-3D model
1	400m from dam base	18.8	17.68	35.57	36.85	21.9	22.18
2	Absolute error	-1.12		1.28		0.28	
3	Relative error (%)	5.96		3.60		1.28	

d. Calculation scenarios

To ensure representativeness in expressing correlations between quantities, we used dimensionless variables to build formulas, and set:

$$\alpha_B = \frac{B_f}{B_{ld}};\ \alpha_{h_f} = \frac{h_f}{H};\ \alpha_{h_h} = \frac{h_h}{H};\ \alpha_{h_w} = \frac{h_w}{H} \text{ và } T = t.\sqrt{\frac{g}{H}}$$

In which: α_B: Break width ratio; α_{h_f}: Break height ratio; α_{h_h}: Downstream water depth ratio; α_{h_w}: intermittent wave height ratio.

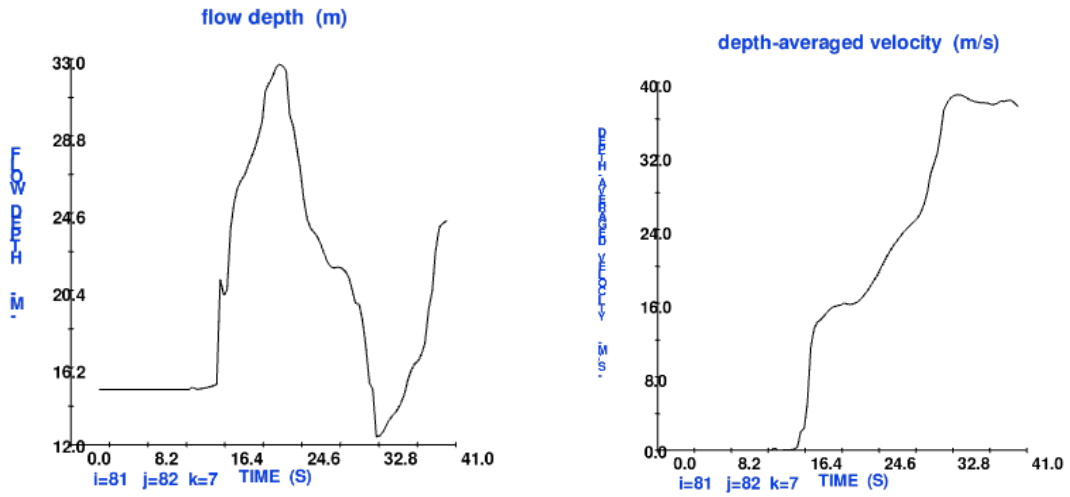

a. Depth of the flow

b. Velocity of the flow

Figure 6: The flow depth and velocity at point x=400m

a. Wave shape on physical model

b. Wave shape on Flow-3D

Figure 7: The downstream wave shape on physical model and Flow-3D model

There were total 20 scenarios including 5 values of α_B = 0.20;0.25;0.5;0.75;1.0 and 4 values of α_{hf} = 0.35,0.5;0.65;0.9. With the assumption that the flow into the lake was negligible and the volume of the breach was much smaller than the volume of the lake bed ($1.5.10^{-3}$ to $6.5.10^{-5}$).

3. RESULTS AND DISCUSSION

In the upstream reservoir, the shape and direction of the wave propagation will depend on the characteristics of the upstream reservoir's shape (ventral shape or wedge shape). In this study, the author studied ventral reservoirs. The image extraction results showed that dam-break waves propagated in two directions: vertical and horizontal. The development of longitudinal wave length and horizontal wave length at the upstream depended on the size of the break (Break width - Bf, break height - hf) and the upstream water level at the time of break.

The process of dam failure occurred quickly and the flow characteristics changed rapidly. In this study, the wave propagation in the upstream reservoir was researched and analyzed from the results of the 3D mathematical model (Flow-3D).

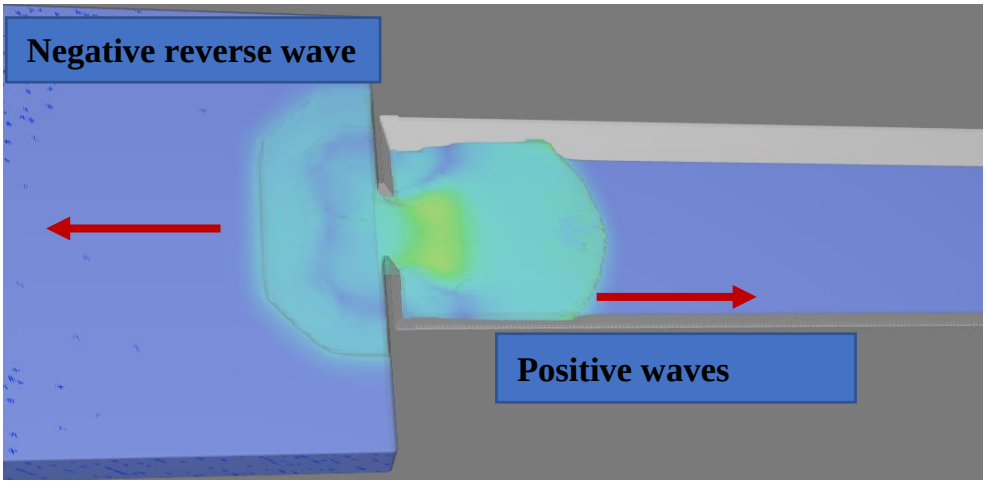

Figure 8: Wave propagation in case of dam break

3.1. Wave shape and dam-break wave propagation at the upstream

Through in-depth analysis and extraction of results of 20 scenarios (αB=0.2÷1.0; αhf=0.35 ÷0.90) as analyzed above, the observation of the flow phenomenon on the upstream reservoir showed that the formation and development of intermittent wave shape divided into two stages:

Stage 1: When dam break wave dynamics had not yet reached the shores on both sides of the reservoir. Using the image extraction and superposition method, combined with AutoCAD software, the upstream intermittent wave shape was ½ Oval - Figure 8.

The intermittent wave image was the image of the concave area before the rupture. Divide the concave area into 2 small areas: area 1 - the flow area before the break and area 2- the area on both sides of the break edge as shown in Figure 11, call the angle created by the straight line passing through the edge of the break and the intersection between area 1 and the break area 2 is β. In the calculation scenarios, simulation angle β ranged from 640 to 680 (angle $\beta=65^0$ appeared most often)

Stage 2: When the interrupted wave hit the shore on both sides, the wave crest was on a straight line, the wave's influence area was rectangular with the width boundary being the shore on both sides and the length boundary from the upstream edge of the break to the first wave crest.

In the calculating case when $\alpha_B>0.5$; and $\alpha_{hf}>0.5$, beside reverse wave-negative, there was reverse wave-positive. The reverse wave-positive appreared after the dam break at T>5.0. Therefore, when T>5.0 reverse wave – negative (in front) and reverse wave-positive (behind) appreared at the same time at the upstream of the reservoir –Figure 9 Max height of the reverse wave – positive was smaller than the height of reverse wave – negative of 0.08H.

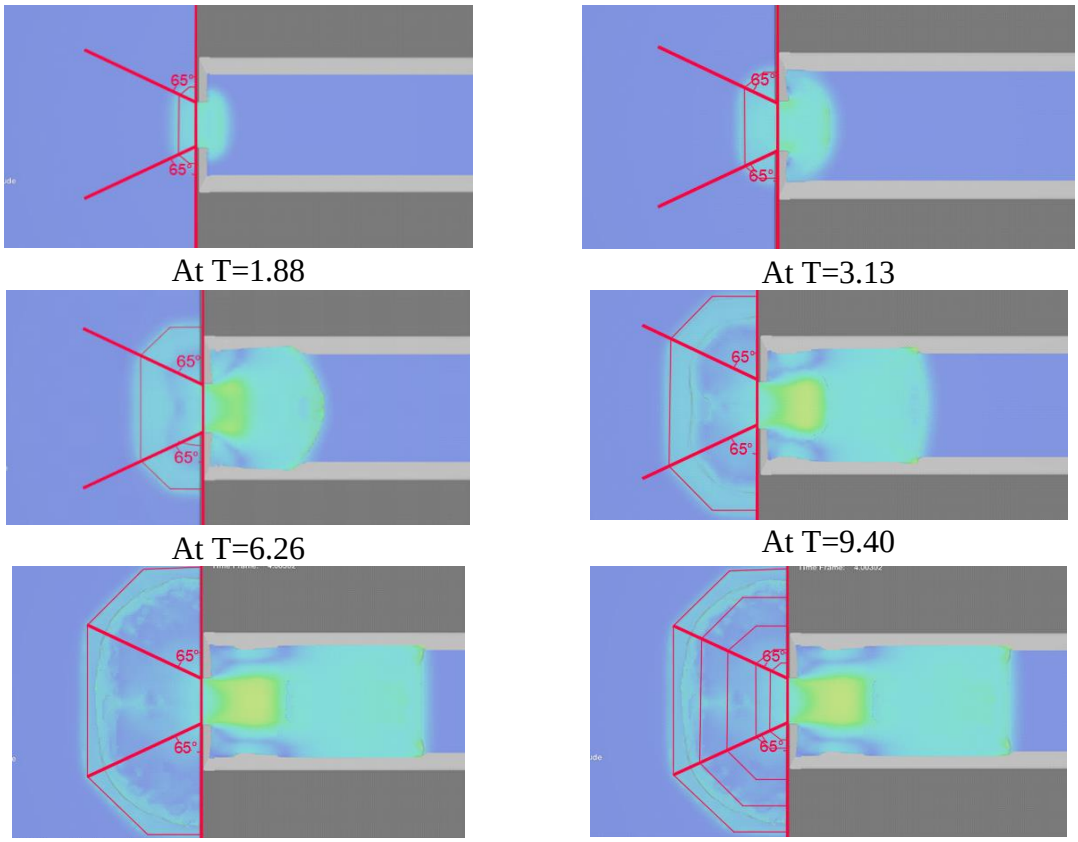

At T=1.88 At T=3.13

At T=6.26 At T=9.40

At T=12.52 Combined times

Figure 9: Upstream wave shape with α_B=0.5 and α_{hf}=1.0

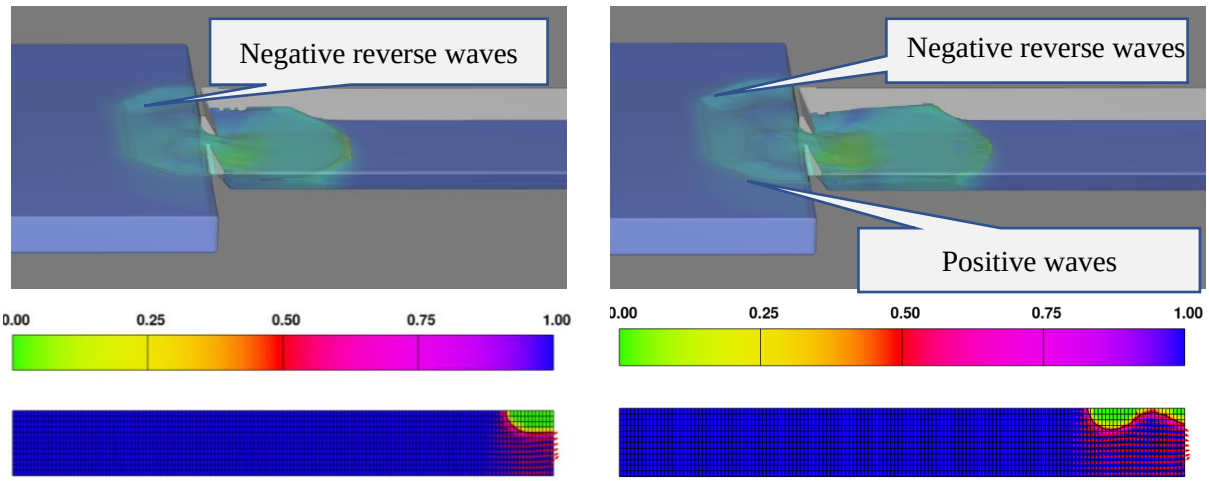

T=5.0- only reverse wave - negative

T=6.26 - Both negative & positive reverse waves

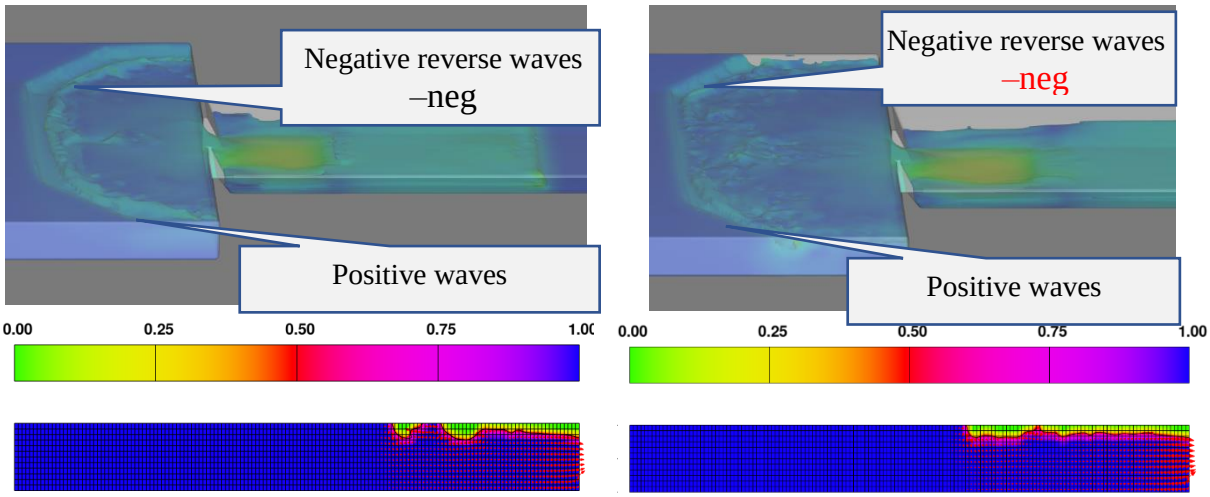

T=12.52 Negative & positive reverse waves T=15.55 Negative & positive reverse waves

Figure 10: The formation and existence of upstream waves

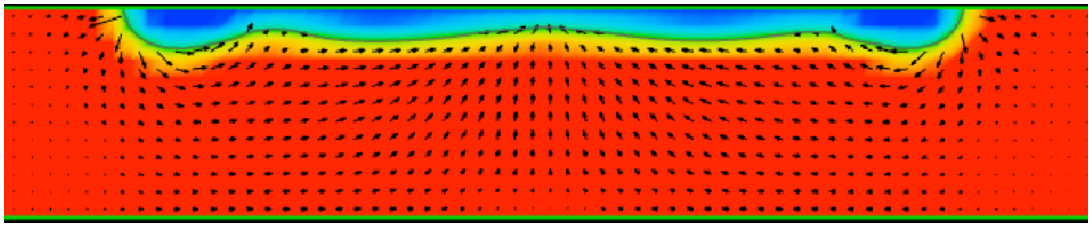

Figure 11: Cross section of the reservoir at X=0.25m

The process of forming a positive reverse wave is explained as follows: At the initial time, the flow from the concave area escaped through the breach. When the dam break time increased (T>5.0), the concave area was opened wide, the surrounding flow ran to the concave area (Figure 11), the flow moving to the concave area increased; The more the concave area developed, the more flow ran in and at the point when the size of the break was no longer able to keep up with the flow from the concave area, causing accumulation and stagnation, increasing the level of water pushed back upstream produced reverse waves. The reverse positive wave then propagated upstream until the flow in the lake completely escaped through the breach

3.2. Relationship between horizontal wave width, longitudinal wave length and the crack size

To determine the relationship between intermittent wave length and width in the upstream of the reservoir, we first divided the wave shape (on the plane) at a time T into two areas. Area 1 was the area before the break (tended to expand to both sides), area 2 was the area on both sides of the break. The boundary between area 1 and area 2 created an angle β with the horizontal direction of the rupture (Details are shown in Diagram in Figure 12).

To ensure representativeness in expressing correlations between quantities, we set X=$\frac{L_{sd}}{H}$; Y=$\frac{B_f}{B}$ và $T = t.\sqrt{\frac{g}{H}}$

From the results of calculating 20 scenarios, the thesis extracted, processed, and standardized the data set to establish the relationship X by T corresponding to the values of Y- as shown in Figure 13. From there, we can determine L_{sd} at time T. After having L_{sd}, determine L_{sn} according to formula (8).

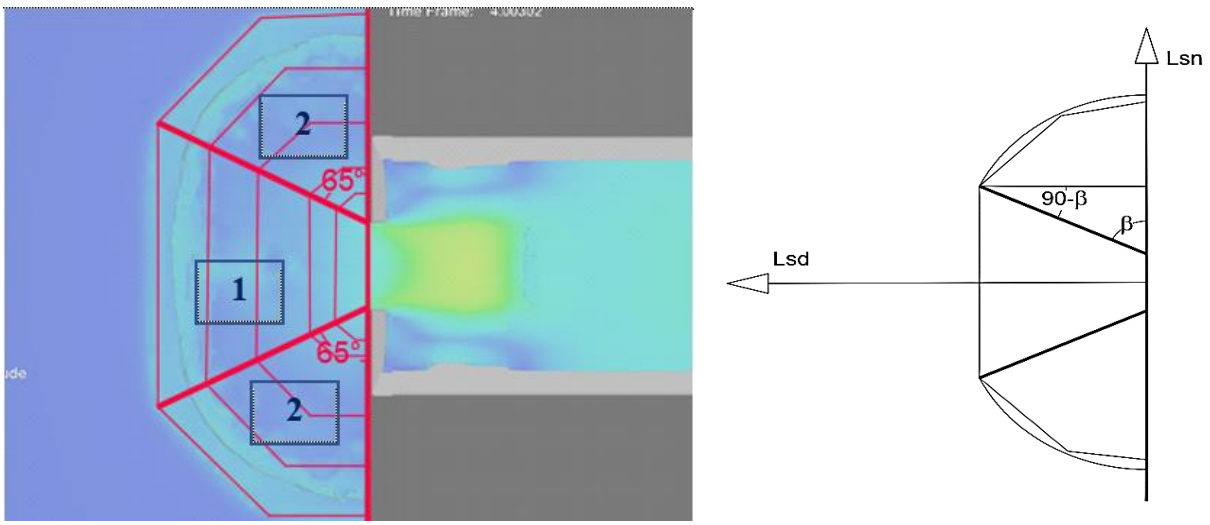

Figure 12: Calculation of longitudinal wave length (L_{sd}) and horizontal wave length (L_{sn})

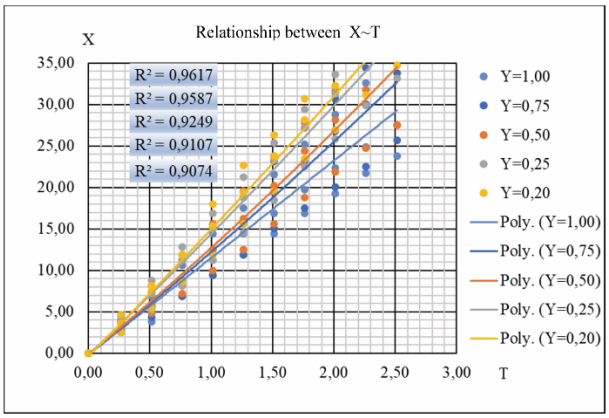

Figure 13: Relationship between X~T by Y

At a time T when determining Lsd, we will determine Lsn according to formula (7).

$$L_{snT} = \frac{B_f}{2} + \frac{LsdT}{\cos(90^0 - \beta)} \quad (7)$$

In the calculated cases, the angle β obtained was in the range of 64° ÷68°. Many calculated and simulated cases determined β=65°. When β~65° formula (7) will be:

$$L_{snT} = 0.5B_f + \frac{L_{sdT}}{\cos(35^0)} = 0.5B_f + 1{,}22x\ L_{sdT} \quad (8)$$

In which: L_{snT} Dam break wave dynamics' width at the time T.

L_{sdT} Dam break wave dynamics' length at the time T.

4. CONCLUSION

"When a dam has incident, negative reverse waves appear upstream of the reservoir, negative reverse waves appear downstream of the reservoir" [1]. However, in some cases of survey and calculation, at a certain time, at the upstream of the reservoir there will simultaneously appear a pair of negative reverse and positive reverse waves moving in the opposite direction to the flow upstream.

On the plane, the scope of wave influence at the upstream is determined according to formula (7) or approximately according to formula (8).

REFERENCES

[1] Nguyen Canh Cam (2006), Open Flow Hydraulics, Construction Publishing House, Hanoi.

[2] Le Van Nghi, Bui Van Huu and associates (2015), "Upstream and downstream risk assessment researches of dam failures of Da river's cascaded hydropower system" KC08.22/11-5. Hanoi

[3] D. Michael Gee, Comparison of Dam Breach Parameter Estimators, Senior Hydraulic Engineer, Corps of Engineers Hydrologic Engineering Center, 2009.

[4] Esmaeeli Mohsenabadi.S, M. Mohammadian, I. Nistor, H. Kheirkhah Gildeh (2019), CFD Modelling of Near-Field Dam Break Flow.

[5] Flow Science Inc. Flow-3D Users Manual; Flow Science Inc.: Santa Fe, NM, USA, 2016.

[6] Gozali.S; Hunt, B (1993), "Dam-break solutions for a partial breach". Journal of Hydraulic Research, IAHR, Vol. 31,1993, No.2, pp. 205-214.

[7] Hatice Ozmen-Cagatay and Selahattin Kocaman (2010), Dam-Break Flow in the Presence of Obstacle: Experiment and CFD Simulation, Turkey

[8] Hatice Ozmen-Cagatay and Selahattin Kocaman (2012), The effect of lateral channel contraction on dam break flows: Laboratory experiment, Turkey.

[9] Hatice Ozmen-Cagatay and Selahattin Kocaman (2020), Experimental and Numerical Analysis of a Dam-Break Flow through Different Contraction Geometries of the Channel, Turkey.

[10] Hunt, B. (1982), "Asymptotic Solution for Dam-Break Problem". Journal of the Hydraulics Division, ASCE, Vol. 108, No. HY1, pp. 115-125.

[11] Hunt, B. (1984), "Perturbation Solution for Dam-Break Floods". Journal of Hydraulic Engineering, ASCE, Vol. 110, No. 8, pp. 1058-1071.

[12] Hunt, B. (1987), "An Inviscid Dam-Break Solution". Journal of Hydraulic Research, IAHR, Vol. 25, No. 3, pp. 313-327.

[13] Hunt, B. (1989), "The Level-Reservoir Approximation for Unsteady Flows on Sloping Channels". Journal of Hydraulic Research, IAHR, Vol. 27, No. 3, pp. 347-354.

[14] Ritter, A. (1892), "The Propagation of Water Waves". Ver. Deutsch Ingenieure Zeitschr. (Berlin), Vol. 36, Pt. 2, No. 33, pp. 947-954.

[15] Stoker, J. J. (1957), "Water Waves. Interscience Publishers", New York.